

Laser multi-layer cladding on ZM6 magnesium base alloy

Changjun Chen (陈长军), Dongsheng Wang (王东生), and Maocai Wang (王茂才)

State Key Laboratory for Corrosion and Protection, Institute of Metal Research,
Chinese Academy of Sciences, Shenyang 110016

Received August 12, 2002

A pulsed Nd: YAG laser is used in multi-layer cladding on ZM6 Mg base alloys. The microstructure is studied with an optical microscope and a scanning electron microscope (SEM). The composition within the layer was determined by electron probe microanalysis (EPMA). X-ray diffraction (XRD) was also used to investigate the phase of constituents of the cladding zone. The results show that microstructure in solidified cladding layer changes much when treated by high energy laser beam. The microstructure of the ZM6 alloy consists of α -Mg and Mg₉Nd, while the L-ZM6 of α -Mg, Mg₉Nd and α -Zr. The depth of the cladding is over 1 mm. Many fine particles were found to be distributed homogeneously throughout the matrix and the columnar grain grows along substrate.

OCIS codes: 140.0140, 350.0350, 140.3390, 350.3390.

Mg base alloys are being increasingly used in varied areas of industry due to their low densities. A major obstacle to the use of Mg base alloys in structural application is their poor corrosion resistance. When coupled with a noble metal, magnesium undergoes anodic dissolution and hence exhibits poor resistance. For example, the fro-supporting aero-engine house (ZM2) is coupled with a noble metal (1Cr₁₁Ni₂W₂Mo), which lead to corrosion pits on its surface. The depth of the corrosion pits varies from 0.1 to 1.0 mm.

In the past, various methods have been tried to enhance the surface properties of Mg base alloy, but there still exist much problems such as high melting oxide layer at the surface, the strong heat dissipation from the treating region, oxidation, porosity, cracking, ignition and insufficient depth, etc. reported by Si^[1].

Laser treatment is an efficient way to improve the corrosion resistance of Mg base alloys. Wang *et al.*^[2,3] have performed the laser cladding of Mg-Al alloy or Mg-Zr alloy powder on magnesium. In order to overcome the oxidation problem and the high vapor pressure-related problems, a complex vacuum apparatus was adopted. R. Galun *et al.*^[4] have investigated the feasibility of laser surface alloying of Mg base alloys with Al, Cu, Ni and Si. The hardness can be increased to values above 250 HV, but the alloying depth only varied from 700 μm to 1200 μm . We have reported the laser multi-layer cladding on ZM2 and ZM5 Mg-base alloys^[5]. In this paper, a pulsed Nd: YAG laser was used to clad layer by layer for repairing the pits/faults of die casting ZM6 alloys with the purpose of repairing the finished products used in air-engine.

Die casting plates of ZM6 alloy was used as target for laser multi-layer cladding. The chemical composition is 0.2% – 0.7% Zn, 0.4% – 1.0% Zr, 2.0% – 2.8% Re (with more than 85% Nd), 0.10% Cu (Max), 0.01% Ni, 0.30% impurities; the others are Mg (wt-%). In order to simulate the pits/faults of finished products used in aero-engine, the artificial faults such as pit, cave-in and groove were formed on the same samples. All the faults were over 1 mm depth. The plate was polished with 600-grit SiC paper and cleaned prior to laser multi-layer cladding.

Laser multi-layer cladding was carried out with a pulsed JJ-D-400 Nd:YAG laser with wavelength of 1.06 μm and power of 400 W. The focal spot diameter was 1.5 – 2.0 mm. Pulse width of 4.0 ms, the plus frequency of 5 Hz and the focusing optics with focal length of 230 mm were employed. The surface was scanned at velocities between 3 and 5 $\text{mm}\cdot\text{s}^{-1}$, adjacent scans being partially overlapped by 40% – 60%. A continuous coaxial flow of high purity of argon was used to protect the surface of the specimens and the melted pool was shielded with argon gas delivered by means of a 3 mm copper nozzle inclined at 35°C. These parameters were chosen because for laser power of below 300 W, a scanning velocity of less than 3 $\text{mm}\cdot\text{s}^{-1}$ was required to melt the cladding material thoroughly, and this might result in overheating of the substrate material. On the other hand, if the laser power higher than 500 W was used, a scanning velocity of over 5 $\text{mm}\cdot\text{s}^{-1}$ was required to avoid over-melting of the substrate. The focusing optics, the number of pulse per step and the overlapping percent between two successive laser pulses influence the condition of the multi-layer cladding. Evaporation was observed for all laser processing conditions.

After the processing, the cross-section of the specimen was observed with an optical microscope, a scanning electron microscope (SEM), and a composition analysis was made by an electron probe microanalysis (EPMA). Linescans were carried out across the laser cladding layer to determine the distribution of the elements within the layer. X-ray diffraction was also used to identify formed intermetallic compounds.

Figure 1 is the morphology of the multi-layer cladding, and shows that the depth of the cladding is over 1 mm. Figure 2 shows the interface between the cladding zone and the substrate. The substrate is identified as *S* and cladding region as *L*. The interface is marked as *I*. The good fusion between the clad and the substrate can be seen. And there is no porosity, cracking, etc. on the interface and in the cladding zone. Moreover, no oxidation has occurred in the cladding layer.

The reason why the laser cladding alloy (L-ZM6) exhibited a distinct feature of second electron image compared from ZM6 alloy is that the laser cladding technique

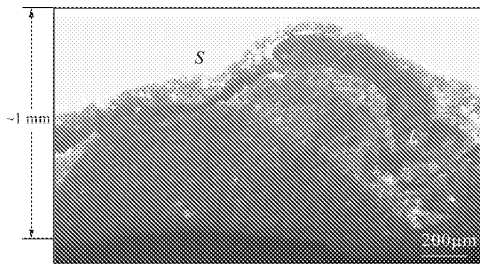


Fig. 1. Morphology of the multi-layer cladding.

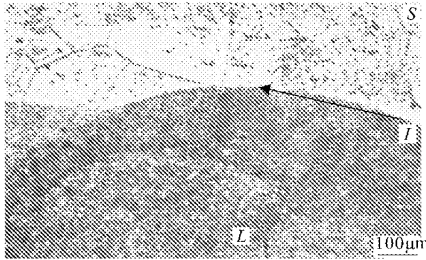


Fig. 2. Interface between the substrate and the cladding zone.

provides a unique means of synthesizing non-equilibrium alloys due to its inherent rapid solidification rate, which promotes the formation of either an amorphous phase or non-equilibrium crystalline phases^[6]. The attributes of rapid solidification to the multi-layer cladding on ZM6 can be conveniently summarized: microstructure refinement, extension of solubility limits, and formation of non-equilibrium crystalline or amorphous phase^[7]. In ZM6 alloy, for example, laser cladding increases the saturation of Zn/Zr/Nd in α -Mg solid solution^[8].

The concentration of Mg, Zr, Zn and Nd in the cladding zone was determined by EPMA (Fig. 3). Large variations of Zr concentrations were found both within the substrate and the cladding zone. A relatively steady Mg and Nd concentrations, however, were found within the cladding zone while large variations were found in the substrate, indicating a better distribution of Mg and Nd in the cladding zone. The measurement in the cladding layer indicated that there is no significant difference of the average concentration of Zn within the substrate and the cladding zone. Linescans in the laser cladding zone and at the substrate/melt pool interface failed to reveal any significant difference of oxygen concentrations across the cladding layer.

Figure 4 shows an XRD pattern of the specimen. From Fig. 4(a), it is identified that ZM6 alloy consisted of α -Mg and Mg_9Nd , while the L-ZM6 consisted of α -Mg, Mg_9Nd and α -Zr (see Fig. 4(b)). The reason why the different phases formed in ZM6 and in L-ZM6 alloy could be that the pulse laser inherent rapid solidification rate results in synthesizing non-equilibrium alloy and creating a fine dispersion of intermetallic phases^[6,9,10]. The observation on surface of the cladding zone showed that the surface was darkened, but no magnesium oxide or nitride was detected by XRD.

This work was supported by Shenyang Liming Aero-engine Group Corporation AVIVI under Grant No. 00-04-06. C. Chen's e-mail address is chjchen@imr.ac.cn.

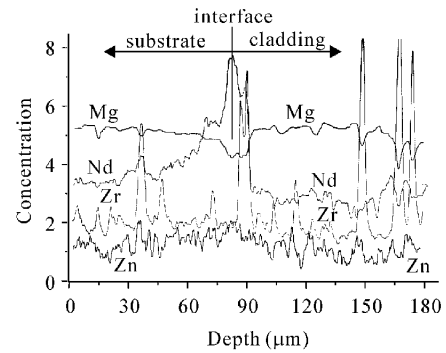


Fig. 3. Mg, Nd, Zr and Zn concentration profile across the laser melted layer.

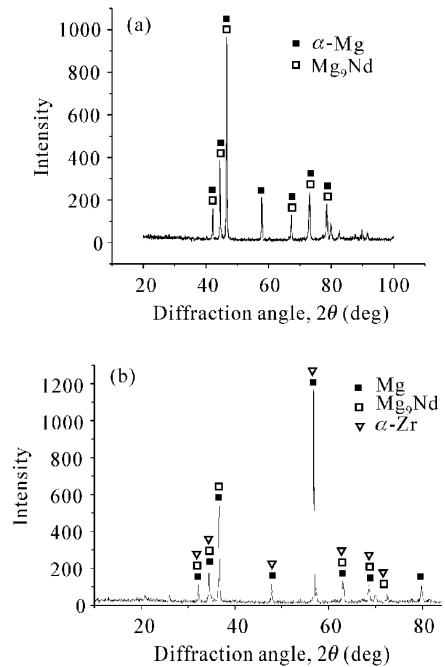


Fig. 4. X-ray diffraction profiles, (a) ZM6 and (b) L-ZM6.

References

1. C. Y. Si, *Welding Handbook*, Vol. 2 (in Chinese) (Mechanical Industry Press, Beijing, 1992) p. 521.
2. A. A. Wang, S. Sircar, and J. Mazumder, *J. Mater. Sci.* **28**, 5113 (1993).
3. R. Subramanian, S. Sircar, and J. Mazumder, *J. Mater. Sci.* **26**, 951 (1991).
4. R. Galun, A. Weisheit, and B. L. Mordike, *J. Laser Applications* **8**, 299 (1996).
5. C. J. Chen, D. S. Wang, W. Y. Guo, and M. C. Wang, *Appl. Laser* (in Chinese) **22**, 76 (2002).
6. F. H. Froes, Y.-W. Kim, and S. Krishnamurthy, *Mater. Sci. and Eng.* **A117**, 19 (1989).
7. F. Hehmann, F. Sommer, H. Jones, and R. G. J. Edyvean, *J. Mater. Sci.* **24**, 2369 (1989).
8. G. L. Makar, J. Kruger, and K. Sieradzki, *Corrosion Science* **34**, 1311 (1993).
9. M. Bamberger, *Mater. Sci. and Technol.* **17**, 15 (2001).
10. I. J. Polmear, *Mater. Sci. and Technol.* **10**, 1 (1994).